The fatal fungal outbreak on Vancouver Island is characterized by enhanced intracellular parasitism driven by mitochondrial regulation

Hansong Ma[a], Ferry Hagen[b,c], Dov J. Stekel[a], Simon A. Johnston[a], Edward Sionov[d], Rama Falk[d], Itzhack Polacheck[d], Teun Boekhout[b,c], and Robin C. May[a,1]

[a]School of Biosciences, University of Birmingham, Edgbaston, Birmingham B15 2TT, United Kingdom; [b]CBS Fungal Biodiversity Centre, Royal Netherlands Academy of Arts and Sciences, Uppsalalaan 8, NL-3584CT, Utrecht, The Netherlands; [c]Division of Acute Medicine and Infectious Diseases, University Medical Center Utrecht, NL-3508GA, Utrecht, The Netherlands; and [d]The Department of Clinical Microbiology and Infectious Diseases, Hadassah-Hebrew University Medical Center, Ein Kerem, Jerusalem 91120, Israel

Edited by Joan Wennstrom Bennett, Rutgers, The State University of New Jersey, New Brunswick, NJ, and approved June 19, 2009 (received for review March 19, 2009)

In 1999, the population of Vancouver Island, Canada, began to experience an outbreak of a fatal fungal disease caused by a highly virulent lineage of *Cryptococcus gattii*. This organism has recently spread to the Canadian mainland and Pacific Northwest, but the molecular cause of the outbreak remains unknown. Here we show that the Vancouver Island outbreak (VIO) isolates have dramatically increased their ability to replicate within macrophages of the mammalian immune system in comparison with other *C. gattii* strains. We further demonstrate that such enhanced intracellular parasitism is directly linked to virulence in a murine model of cryptococcosis, suggesting that this phenotype may be the cause of the outbreak. Finally, microarray studies on 24 *C. gattii* strains reveals that the hypervirulence of the VIO isolates is characterized by the up-regulation of a large group of genes, many of which are encoded by mitochondrial genome or associated with mitochondrial activities. This expression profile correlates with an unusual mitochondrial morphology exhibited by the VIO strains after phagocytosis. Our data thus demonstrate that the intracellular parasitism of macrophages is a key driver of a human disease outbreak, a finding that has significant implications for a wide range of other human pathogens.

cryptococcus | macrophage | Vancouver Island outbreak | virulence

For many pathogens, intracellular survival is critical to their pathogenicity, because it provides a basis for dissemination and latency. Intracellular pathogens are able to spread within the body, triggering little or no effective immune response from the host. Moreover, many pathogens use the host cell as a nutrient source to support rapid replication, thus acting as genuine intracellular parasites (1, 2). The human fungal pathogen *Cryptococcus* is an intracellular parasite of macrophages (3, 4) and is believed to exploit these host cells to traffic from the lung, the primary site of infection, into the central nervous system (5, 6).

There are two pathogenic species within the *Cryptococcus* genus: *C. neoformans* and *C. gattii*. They are the causative agents of cryptococcosis, a fatal infection of the central nervous system in humans. Globally, the vast majority of cryptococcosis cases occur in immunocompromised patients and are caused by *C. neoformans*. In contrast, *C. gattii* typically infects immunocompetent individuals but causes only 1% of cryptococcosis cases worldwide and has thus been significantly understudied (7). However, the ongoing outbreak of *C. gattii* infection in immunocompetent individuals on Vancouver Island and the recent spread of this outbreak to mainland British Columbia and the Pacific Northwest (8–10) have dramatically increased global concern about this pathogenic species. Previous amplified fragment length polymorphism (AFLP) and multilocus sequence typing (MLST) studies have demonstrated that the Vancouver Island outbreak (VIO) is mainly caused by a single, hypervirulent genotype of *C. gattii* (AFLP6A/molecular type VGIIa) (8). Intriguingly, this genotype is not restricted to Vancouver Island but is also shared by, for instance, the CBS6956 strain (also known as NIH444 or ATCC32609, isolated from a patient in Seattle in 1971) and CBS7750 (isolated from a *Eucalyptus* tree in San Francisco in 1992) (11, 12), suggesting that a recent genetic change has occurred within the VIO lineage, potentially as a result of an unusual same-sex mating event (12). However, the underlying molecular cause for the hypervirulence of this lineage remains unknown.

Results

Hypervirulence of VIO Strains Is Not Directly Linked to Any Known Virulence Factors. To study the cause of hypervirulence within the VIO isolates, we undertook a high-throughput analysis of well-characterized virulence traits (capsule size, melanization, phospholipase production, proteinase production, and other enzymatic activities) in 39 *C. gattii* strains representing both VIO and non-VIO isolates (Table S1 and Table S2). However, there was no consistent difference between VIO and non-VIO isolates belonging to this genotype in any of the traits tested, suggesting that the virulence of VIO strains does not simply result from over-expression of these individual cryptococcal pathogenicity factors. Such a finding is consistent with recent data suggesting that many cryptococcal virulence genes/factors remain to be discovered (13).

VIO Strains Show Enhanced Intracellular Parasitic Capacity Compared to Other *C. gattii* Strains. Given the importance of macrophage parasitism in cryptococcal infection, we developed an in vitro method to monitor intracellular yeast number for 64 h following phagocytosis by murine macrophage-like cells J774 (see experimental procedures). We then used intracellular proliferation rate (IPR, which was calculated by dividing the maximum intracellular yeast number by the initial intracellular yeast number at T_0) as a parameter to quantify the relative level of intracellular parasitism between strains. Based on this method, we calculated average IPR for 55 strains, including 16 *C. neoformans* and 39 *C. gattii* isolates (Table S1). Strikingly, all of the VIO AFLP6A isolates exhibit much higher intracellular proliferation rates compared to other *C. gattii* strains, including AFLP6A strains isolated from other areas of the world (Fig. 1*A*). Time-lapse microscopy of J774 macrophages infected with each of the *C. gattii* strains confirmed the high IPR values observed among VIO strains (Movies S1–S3). Importantly,

Author contributions: H.M., I.P., T.B., and R.C.M. designed research; H.M., F.H., S.A.J., E.S., R.F., and I.P. performed research; F.H., D.J.S., I.P., and T.B. contributed new reagents/analytic tools; H.M., F.H., D.J.S., S.A.J., I.P., T.B., and R.C.M. analyzed data; and H.M. and R.C.M. wrote the paper.

The authors declare no conflict of interest.

This article is a PNAS Direct Submission.

[1]To whom correspondence should be addressed. E-mail: r.c.may@bham.ac.uk.

This article contains supporting information online at www.pnas.org/cgi/content/full/0902963106/DCSupplemental.

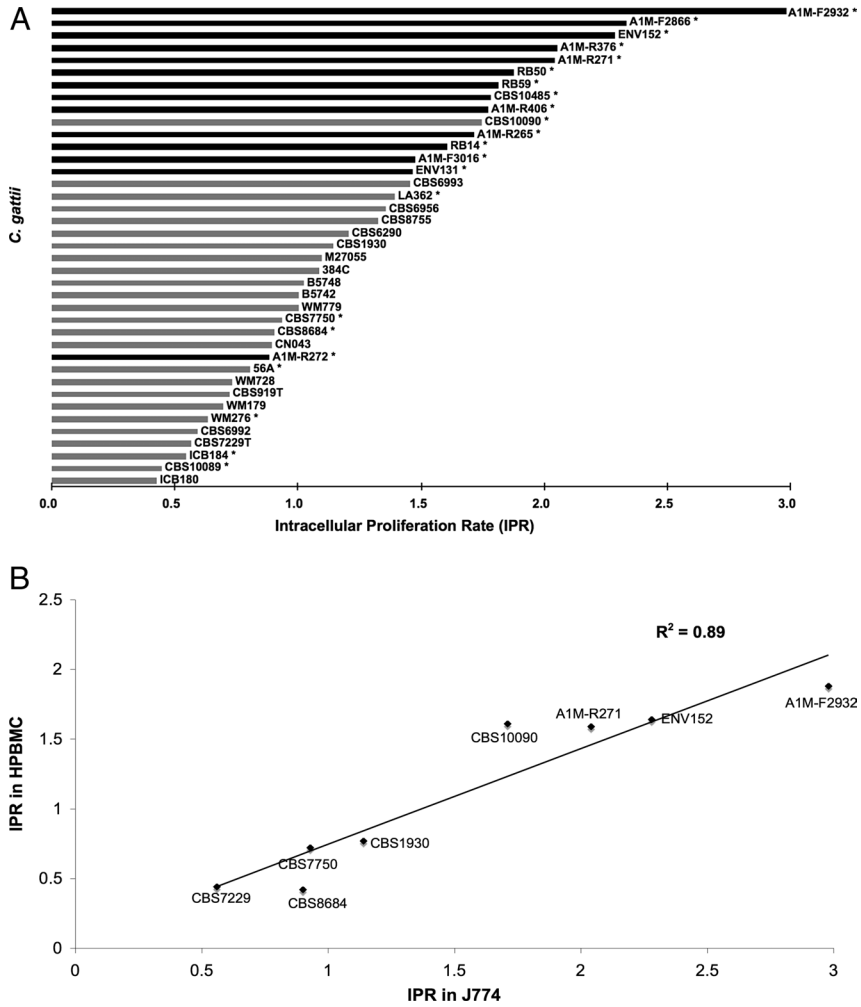

Fig. 1. (*A*) Significant inter-strain variation in IPR occurs within the *C. gattii* species ($n = 39$). Black bars represent VIO isolates, which proliferate far better than other *C. gattii* strains (gray bars). The only exception was A1M-R272, which belongs to the minor (AFLP6B) group of the outbreak and has previously been shown to be less virulent than other VIO strains (12). An asterisk (*) denotes strains used for the microarray study. (*B*) IPR values of 8 strains in human primary blood-derived macrophage cells (HPBMCs) correlate significantly with those observed in J774 ($P = 0.00044$, Spearman's test, $n = 8$). The IPR values obtained with HPBMC are generally lower than those seen in J774 macrophages, which may be a result of the higher cryptococcal expulsion rates observed in primary cells, as previously reported (36).

this phenomenon is not specific to the J774 mouse cell line, because the VIO strains also show enhanced intracellular proliferation in human primary macrophages derived from peripheral blood (Fig. 1*B* and Table S4). This proliferative capacity appears to reflect specific parasitism of the live macrophage, rather than simply enhanced utilization of nutrient sources available in the host cell, since the VIO strains do not show significantly higher growth rates when grown in mammalian cell lysates (Table S5). Thus the VIO strains share a common capacity to act as intracellular parasites that is unique to this pathogen population.

Intracellular Proliferation Rate Predicts Virulence of Cryptococcal Strains in a Murine Model of Cryptococcosis. Several early studies have highlighted the hypothesis that macrophages may exacerbate cryptococcal infection in mice. Alveolar macrophage depletion was associated with amelioration of disease in three murine strains as measured by lung fungal burden (14), and decreased the dissemination of a glucosylceramide-deficient mutant of *C. neoformans* in immunodeficient mice (15). We therefore tested whether high intracellular proliferation capacity is linked to the hypervirulence of the VIO lineage. To do this, IPR values were compared with both published and newly-generated mouse median survival times (ST_{50}). Remarkably, IPR and murine ST_{50} are highly significantly correlated ($P = 0.00017$, linear regression, Fig. 2): a correlation that holds true for both *C. neoformans* and *C. gattii* and is independent of the mouse model used. In other words, the ability to survive and proliferate inside a host macrophage contributes significantly to cryptococcal virulence in the murine model and presumably also in infected humans, as suggested by the human primary macrophage data. This previously undiscovered link between intracellular proliferation rate and virulence also provides a possible explanation for why "ancestral" AFLP6A strains share the VIO genotype and yet do not lead to disease outbreaks. For example, CBS6956, which is considered as the potential origin of the AFLP6A subtype (11), shows only a moderate IPR value of 1.35 (Fig. 1*A* and Table S1), indicating that it cannot exploit the intracellular macrophage niche as successfully as the VIO isolates.

Identification of Genes Associated with Enhanced Intracellular Parasitism. Statistical analysis confirmed that the high IPR values exhibited by the VIO isolates did not result from increased expression of any of the known virulence factors analyzed above (Table S2*B*) nor was it due to better utilization of macrophage nutrients (Table S5). Therefore to investigate the molecular basis of enhanced intracellular proliferation, and thus hypervirulence, in the VIO isolates, we used custom-designed *C. gattii* whole-genome tiling microarrays to conduct transcriptional profiling of 24 *C. gattii* strains (21 AFLP6 and 3 AFLP4 isolates) recovered from within J774 macrophages. These strains are genetically very similar but show a wide range of IPR values (Fig. 1*A*). RNA samples from each strain were isolated from intracellular cryptococcal cells 24 h after infection and competitively hybridized against a pooled sample containing equal quantities of RNA from all 24 strains. At this time point, the intracellular number reaches the peak for the majority of strains. Linear regression identified 1,367 target loci in the genome of AFLP6 strains whose expression showed a significant correlation

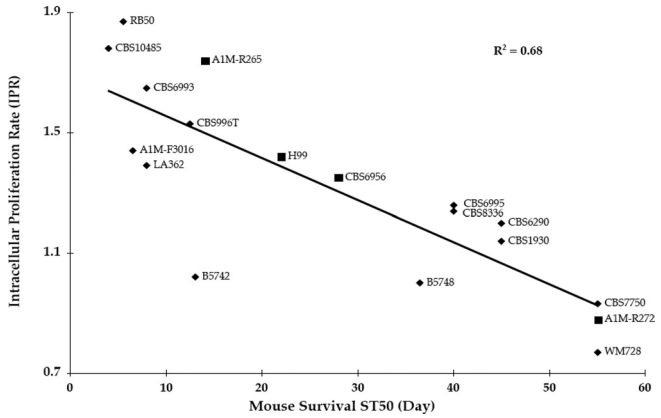

Fig. 2. A significant correlation between mouse survival data [both previously published in ref. 12 (■) and newly generated (◆)] and intracellular proliferation rate (IPR). Mice survived longer when infected with strains with low IPR values as compared with animals infected with high IPR strains ($P = 0.00017$, linear regression, $n = 18$). For the unpublished mouse survival assays, experiments were conducted as described in the *Materials and Methods* section. Published mouse survival data are taken from Fraser et al. (12). Note that strain WM276 has been omitted from the graph, since published ST_{50} values on this strain vary widely for reasons that are not currently understood (12, 45). For strains that did not cause mortality of 50% or more within the 45-day timeframe of the experiment, we arbitrarily assigned an ST_{50} of 55 days.

with IPR values. Two hundred twenty-four of these have predicted function annotations, most of which can be categorized into one of five groups: carbohydrate metabolism, stress response, vesicle/vacuole fusion and transport, protein degradation and synthesis, and nucleotide metabolism (Table S3). Interestingly, although our phenotypic analysis demonstrated that no single known virulence factor was responsible for the hypervirulence of the VIO isolates, several of these genes (e.g., *PLB1*, *CRG1*, capsule related genes, and genes on the mating type locus,) showed a significant expression correlation with IPR, suggesting that they may synergistically contribute to virulence within the AFLP6 lineage. Notably, some of our uncharacterised candidate genes were also recently identified by Liu et al. as influencing melanin and capsule production and, thus, cryptococcal infectivity (e.g., *COP9* signalosome complex and ubiquitin carboxyl-terminal hydrolase) (13).

Due to poor annotation of the *C. gattii* genome, BLAST searching did not identify the function of most of the candidate genes we identified (Table S3). We therefore mapped the genomic distribution of all of the microarray hits by localizing them on the 28 supercontigs of A1M-R265 genome. The distribution was homogenous across all supercontigs, with the remarkable exception of supercontig 25, corresponding to the mitochondrial genome (mtDNA), which was 10-fold overrepresented (Fig. 3*A*, $P = 10^{-24}$, χ^2 test). Quantitative PCR demonstrated that the observed overrepresentation of mitochondrial sequences is not due to an increase in mtDNA copy number, because AFLP6 strains showing very different IPR values nonetheless have similar mtDNA/genomic DNA ratios (Table 1). In addition, mtDNA copy number does not change significantly following intracellular replication, eliminating this as a possible explanation for the overrepresentation of mitochondrial hits (Table 1). Furthermore, the expression of many nuclear-encoded proteins that function in mitochondria is also up-regulated in the VIO strains (e.g., respiratory genes and mitochondrial proteins, Table S3), which is particularly relevant given early in vivo transcriptional profiling showing the high expression of several respiratory genes by this yeast at the site of a central nervous

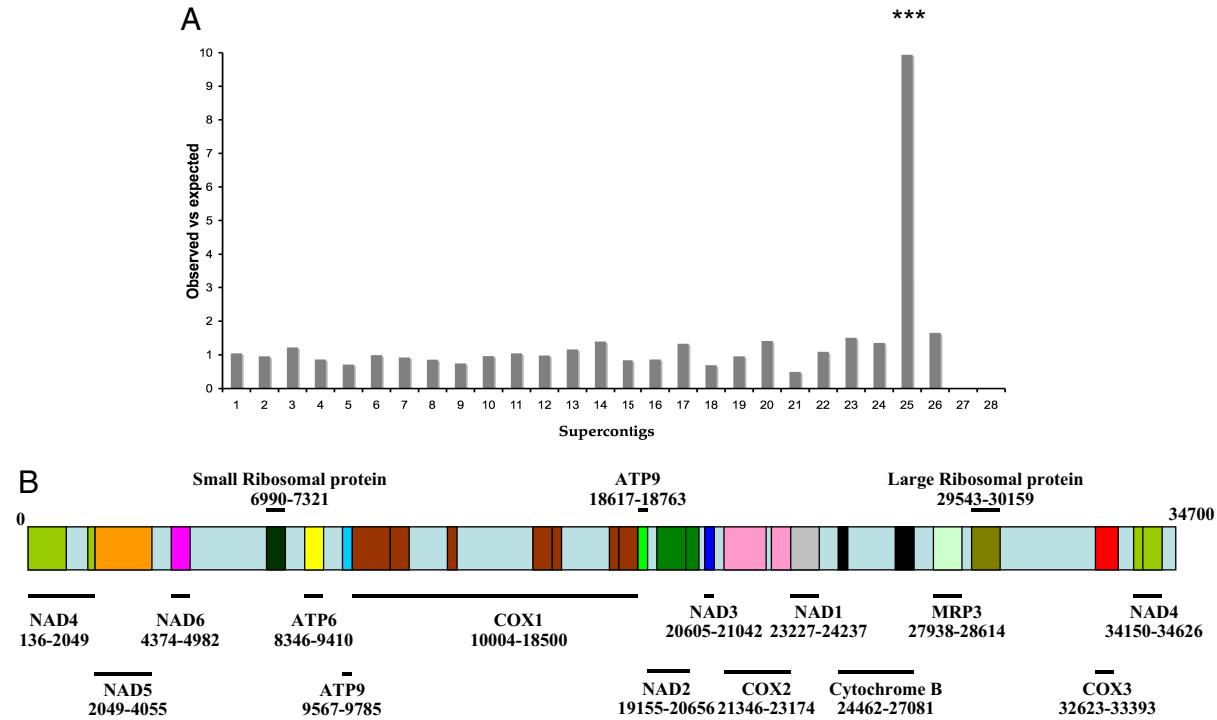

Fig. 3. (*A*) A1M-R265 Supercontig 25 is highly over-represented in the transcriptional analysis ($P = 10^{-24}$, χ^2 test). Probes (1,367) whose expression showed significant correlation with IPR were mapped onto the 28 supercontigs of the A1M-R265 genome and compared to the expected hit rate (assuming a random probe distribution) using the χ^2 test. Supercontig 25 is 10-fold over-represented. (*B*) The predicted genome structure of A1M-R265 supercontig 25. The genome is 34.7 kb in size and, as with other cryptococcal mitochondria, encodes 17 genes important for mitochondrial function and protein synthesis. The ORFs were predicted using Open Reading Frame Finder at NCBI (http://www.ncbi.nlm.nih.gov/gorf/gorf.html) in combination with alignment to the H99 mitochondrial sequence (available at http://www.ncbi.nlm.nih.gov/entrez/viewer.fcgi?db = nucleotide&val = AY101381). The supercontig represents the whole mitochondrial genome of A1M-R265. Sections with light blue color are either introns or intergenic spaces, both of which are substantially expanded relative to *C. neoformans* H99.

Table 1. Real-time PCR to quantify mtDNA copy number per cell

Strains	RT-cycle difference between mitochondrial and nuclear loci	
	Intracellular yeast cells	Yeast cells grown in YPD at 25°C
ENV152	9.75 ± 1.01	9.77 ± 0.61
A1M-R271	8.74 ± 0.38	10.68 ± 1.04
CBS7750	9.44 ± 0.19	10.14 ± 1.59
CBS8684	10.71 ± 0.63	10.44 ± 0.53

Cryptococcal mtDNA copy number (ranging from 400–1,600 copies per cell) does not vary among different AFLP6 strains (2 VIO isolates and 2 other AFLP6 strains) or change following intracellular replication within host macrophages.

system infection (16, 17). Taken together, we propose that mitochondrial function is critical for the virulence of this lineage.

Mitochondrial Morphology Changes in VIO Strains Following Phagocytosis. Given the overrepresentation of mitochondrial genes in the VIO strains, we analyzed the morphology of cryptococcal mitochondria both before and after phagocytosis. Surprisingly, we observed a striking difference in mitochondrial morphology between the VIO and non-VIO strains following intracellular parasitism. During in vitro growth either at 25 °C with shaking in YPD or 37 °C in DMEM + 5% CO_2 without shaking, more than 95% of cryptococcal cells have mitochondria with morphologies that we termed either "diffuse" or "globular" (Fig. 4*A*), regardless of the strain tested. However, after growth inside J774 macrophages, VIO strains developed a tubular mitochondrial morphology (Fig. 4*C*) that was rarely exhibited by non-VIO isolates ($P < 0.0001$, χ^2 test for VIO versus non-VIO strains). Remarkably, the percentage of cryptococcal cells exhibiting tubular mitochondria shows a strong, linear correlation with IPR (Fig. 4*B*, $P = 0.00021$, linear regression), a relationship that raises the possibility of accurately predicting the virulence of cryptococcal genotypes based on a simple, 1-step observation of mitochondrial morphology.

Mitochondrial tubular morphology is generally thought to result from mitochondrial fusion, a phenomenon that allows mitochondria within a cell to cooperate with each other (18) and protects cells from the detrimental effect of mtDNA mutations by allowing functional complementation of mtDNA gene products (19). Moreover, mitochondrial fusion has been found to protect cells from cell death (20, 21). It therefore appears likely that the altered mito-

A

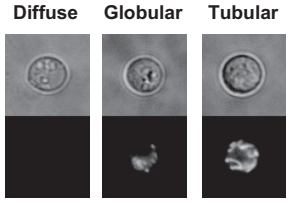

Strains	Diffuse	Globular	Tubular	Total	Percentage of tubular	IPR values
CBS8684	15	46	0	61	0%	0.90
CBS7750	9	58	4	71	6%	0.93
CBS1930	10	44	6	60	10%	1.14
A1M-R271	7	32	24	63	38%	2.04
ENV152	11	28	39	78	50%	2.25
A1M-F2932	14	21	54	89	61%	2.98

B

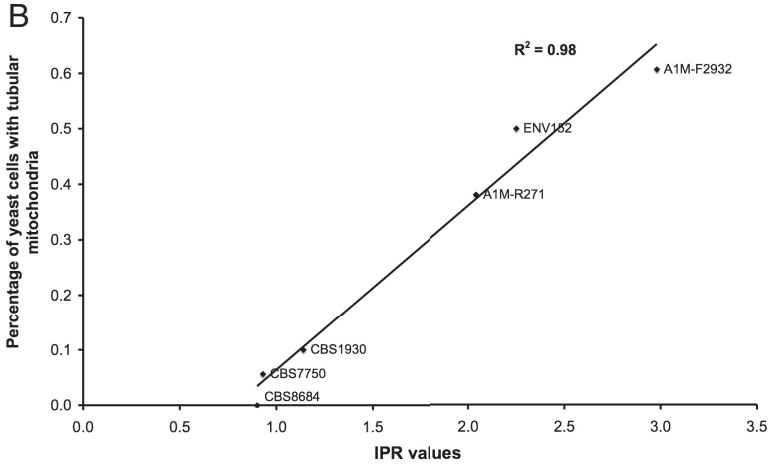

C

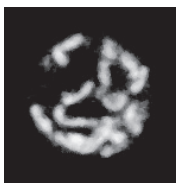

Fig. 4. Vancouver Island Outbreak isolates acquire a characteristic mitochondrial morphology after intracellular growth. (*A*) Representative images of the 3 different mitochondrial morphologies observed (diffuse, globular, and tubular) and a table showing the percentage of intracellular yeast cells with tubular mitochondria in 6 AFLP6 strains (3 VIO and 3 non-VIO isolates). For each strain, a random selection of cryptococcal cells were scored blindly for the 3 different mitochondrial morphologies. Mitochondria with a tubular morphology were found only rarely in strains with low IPR values (non-VIO strains) or in strains (both VIO and non-VIO) that had been grown extracellularly. (*B*) The percentage of intracellular yeast exhibiting a tubular mitochondrial morphology correlates significantly with IPR value ($n = 6$, $P = 0.00021$, linear regression). (*C*) A Z-projection confocal image showing the tubular mitochondrial morphology of a VIO strain. *C. gattii* strain ENV152 (IPR = 2.28), isolated 24 h of growth within J774 macrophages and labeled with MitoTracker.

chondrial gene expression and morphology seen in the VIO strains is a protective response that facilitates rapid intracellular growth and thus enhanced virulence.

Discussion

Our study demonstrates a link between the intracellular parasitism of phagocytes and the virulence of a facultative intracellular pathogen in a murine model of infection. Moreover, we propose that a recent change in mitochondrial regulation within the *C. gattii* lineage has led to an increased intracellular proliferative capacity resulting in the hypervirulent phenotype that underlies the VIO. This change leads to a quantitative linear relationship between intracellular proliferation rate, mitochondrial gene expression, mitochondrial morphology, and virulence.

The mitochondrion, as an essential organelle, has been linked to various cellular activities, such as intermediary metabolism and respiration, cell signaling, iron metabolism, apoptosis, and aging. Nevertheless, its role in modulating virulence of pathogens is unclear. Indeed such a role has been reported only once before, in *Heterobasidion annosum*, which, like *Cryptococcus*, is also a basidiomycete pathogen but of plants rather than animals (22). However, mitochondria can represent a source of rapid evolution of virulence in emerging pathogens because their genomes are present at high copy number and show a mutation rate much higher than that of nuclear DNA (*23–25*). Within the *Cryptococcus* genus, mitochondrial genomes show conserved gene synteny but very different sizes [e.g., 34.7 kb for *C. gattii* (Fig. 3*B*), 32 kb for *C. neoformans* var. *neoformans*, and 24 kb for *C. neoformans* var. *grubii*] (26), indicating that they are under intense selection. This is further supported by recent evidence of mitochondrial recombination in *C. gattii* (27, 28), along with the fact that most of the mitochondrial genetic variation between WM276 (an AFLP4/VGI strain with a low IPR value) and A1M-R265 (a VIO strain with high IPR) lies in coding regions, whilst the intergenic regions are highly conserved.

Mitochondria are dynamic organelles that frequently divide and fuse with each other and it is thought that such behaviors are coordinated with their metabolic function (19). In yeast and mammals, several factors including Drp1/Dnm1 and Mfn/Fzo1 are known to regulate mitochondrial morphology by controlling membrane fission or fusion. Interestingly, we find that *FZO1* is up-regulated in the VIO strains (Table S3) and might therefore contribute to the observed tubular morphology in VIO strains. However, a recent study demonstrated that most fundamental mitochondrial functions, including metabolism and oxidative phosphorylation, are also necessary for the maintenance of tubular networks (29). Hence the tubular morphology is likely to be a result of up-regulation of many candidate genes listed in Table S3. Early studies on *Cryptococcus* have demonstrated the importance of mitochondria in responding to hypoxic conditions and oxidative stress (30, 31). We therefore propose that, after being engulfed by macrophages, the VIO strains are able to promote mitochondrial fusion to form long tubular mitochondria to more efficiently repair mtDNA damage caused by the oxidative species and hypoxic conditions present within the macrophage phagosome.

Since mitochondria are essential for cryptococcal viability (32), attempts to make *petite* (respiratory) mutants have not been successful. In addition, we and others have been unable to mate VGIIa with VGIIα cryptococci to replace the mitochondria of VIO strains with those from less virulent strains (33–35). Therefore, we cannot distinguish whether it is the mitochondrion itself or the regulation of mitochondrial activity via nuclear encoded proteins that is important for the virulence of the VIO lineage. In either scenario, however, mitochondrially-regulated intracellular replication capacity may be a widespread phenomenon in other eukaryotic pathogens and hence an improved appreciation of this process is likely to have significant implications for our understanding of disease epidemics caused by a range of otherwise unrelated pathogens.

Materials and Methods

Yeast Strains and Growth Conditions. All cryptococcal strains used are listed in Table S1. Yeast cells were grown overnight in antibiotic-containing YPD medium (2% glucose, 1% peptone, and 1% yeast extract) with moderate shaking (240 rpm) at 25 °C. Antibiotics were added to the media at the following concentrations: 50 μg/mL ampicillin or 25 μg/mL kanamycin. Yeast cells were collected from the overnight culture by centrifugation at 2,000 rpm for 2 min, then washed with PBS twice, and resuspended in PBS.

Intracellular Proliferation Measurement. A proliferation assay was developed to monitor intracellular proliferation rate of individual strains for a 64-h period following phagocytosis. For this assay, J774 macrophage cells or human primary blood-derived macrophage cells [HPBMCs, which were isolated and activated as previously described (36)] were exposed to cryptococci opsonised with 18B7 antibody for 2 h as described in (36). Each well was washed with PBS 4–5 times to remove as many extracellular yeast cells as possible and 1 mL fresh serum-free DMEM was added. For time point T_0, 1 mL DMEM was discarded and 200 μL sterile dH_2O was added into wells to lyse macrophage cells. After 30 min, the intracellular yeast were released and collected. Another 200 μL dH_2O was added to each well to collect the remaining yeast cells. The intracellular yeast was then mixed with Trypan Blue at a 1:1 ratio and the live yeast cells were counted. For the subsequent 5 time points T_{16}, T_{24}, T_{40}, T_{48}, and T_{64}, both extracellular and intracellular cryptococci were collected and independently counted by hemocytometer in the same manner. For each strain tested, each time course was repeated at least 3 times on different occasions and using different batches of macrophages. Intracellular proliferation rate was calculated by dividing the maximum intracellular yeast number (which is T_{24} for most of the strains) by the initial intracellular yeast number at T_0. We confirmed that Trypan Blue stains 100% of yeast in a heat-killed culture, but only approximately 5% of a standard overnight culture. Compared to conventional colony counting method, this method is more sensitive in detecting the clustered yeast population or yeast cells undergoing budding.

Mitochondrial Staining and Microscopy. Yeast cells, grown overnight in YPD medium at 25 °C at 240 rpm, or grown at 37 °C in DMEM in a 5% CO_2 incubator without shaking for 24 h, or isolated from macrophages 24 h after infection, were harvested, washed with PBS twice and resuspended in PBS containing the Mito-Tracker Red CMXRos (Invitrogen) at a final concentration of 40 nM. Cells were incubated for 30 min at 37 °C. After staining, cells were washed 3 times and resuspended in PBS. For each condition, more than 60 yeast cells for each of the tested strains were chosen randomly and analyzed. For quantifying different mitochondrial morphologies, images were collected on a Nikon Eclipse E300 microscope using 60× oil immersion 1.40NA plan APO objective lens. Both fluorescence images and brightfield images were collected simultaneously. Images were captured with identical settings on a Hammatsu Orca C4745–12NRB with a 0.5× camera lens using Openlab (version 5.5.0; Improvision). All Images were processed identically in Photoshop CS2 (Adobe) and mitochondrial morphologies were analyzed and counted blind. For confocal microscopy, images were collected on a Nikon Eclipse E600 confocal microscope with BioRad Radiance 2000 MP laser scanning system using a 100× oil immersion WD 0.20 objective lens. Images were processed using ZeissSharp2000 software (version 6.0).

Mouse Survival Assay. Yeast inocula [10^6 yeast cells per mouse from a 48-h culture of cryptococci on Sabouraud dextrose agar (SDA) at 30 °C] were injected into the tail veins of male albino BALB/c mice (weight, 20–23 g) by administration of a single bolus injection of a 0.2-mL suspension in PBS. The yeast concentration was determined by counting with a hemocytometer. The viable count was measured as the number of CFU on SDA plates after 24 to 48 h of incubation at 30 °C. With these inocula, systemic infections are regularly produced in mice, and they cause total killing within 5 to 50 days. For each experiment 10 mice were used, maintained in separate cages. The number of surviving animals in each group was recorded daily over a period of 45 days using a blinded experimental design such that animal handlers were unaware of the corresponding IPR value for the strains used. All procedures, care and treatment of mice were in accordance with the principles of humane treatment outlined by the Guide for the Care and Use of Laboratory Animals of the Hebrew University, and were approved by the Committee for Ethical Conduct in the Care and Use of Laboratory Animals (approval number OPRR-A01–5011).

RNA Isolation from Intracellular Cryptococci 24 h After Infection. The phagocytosis assay was carried out as described earlier. After 24 h, extracellular cryptococci were removed with several prewarmed PBS washes and macrophages were lysed with 10 mL ice-cold H_2O for 20 min before being scraped from T75 tissue flasks. The whole mixture was then centrifuged at 1,500 rpm at 4 °C for 5

min and the resulting pellet was washed twice with ice-cold H_2O. Subsequently, the pellet was resuspended in 10 mL H_2O supplemented with 0.05% SDS (SDS) for 5 min to remove macrophage RNA. At this SDS concentration, the macrophages were lysed while cryptococci remained intact and viable (37). The remaining yeast cells were washed 3 times with ice-cold H_2O by centrifugation and resuspension. The final pellet was then used for RNA isolation or frozen at −80 °C until required. Yeast RNA was isolated using Microto-Midi Total RNA Purification System (Invitrogen) in accordance with the manufacturer's instructions.

Microarray Experiment. An Agilent printed whole genome tiling array with 242,003 probes generated against 2 genomes of *C. gattii*, A1M-R265 (Broad Institute) and WM276 (Jim Kronstad), was designed by Oxford Gene Technology (OGT). Average interprobe distance was 140 nucleotides, evenly distributed across both DNA strands. After round 1 of design, any gaps of over 1.5 kb (due to repeat regions, etc.) were then filled using suboptimal probes (700 probes in total) in the same manner. There are 20,212 probes (8.4%) that map onto both genomes.

Using this design, 24 *C. gattii* RNA samples were used to determine differences in their gene expression 24 h after internalisation by macrophages. For the array experiment, RNA samples from each strain were labeled with Cy3, whilst the control, consisting of a pooled sample containing equal quantities of RNA samples from all 24 strains (reference) was labeled with Cy5. See *SI Materials and Methods* for more experimental details.

Microarray Data Analysis. Data were background subtracted using Bayesian method, normalized using Loess normalization (38), and analyzed using the statistical package R (http://www.r-project.org/) based on linear regression against IPR values (an example script is included in the *SI Materials and Methods*). Data were corrected for false-discovery rate (39) before candidates showing q values smaller than 0.086 were BLASTed against both *C. neoformans* and *C. gattii* databases. All hits were also retained for statistical analysis of probe distribution.

Real-Time PCR. Real time PCR using the Sybr Green method was performed on the genomic DNA generated from newly isolated intracellular cryptococci to check the copy number of the mitochondrial genome in comparison to a nuclear region. For the reaction, 4 strains (ENV152, A1M-R271, CBS7750, and CBS8684) were chosen. Every reaction in the experiment was conducted in triplicate. The details of the candidates and primers are listed in the table below.

Candidate loci	Primer 5′	Primer 3′
Nuclear locus	GGTCGAATTGTTCTCAGG	ACCGTCCTTAACCTCGAC
Mitochondrial locus	TTCGTCTTGCTGGTCGACTT	TGGGAGTTGTTGATCGTTG

Phenotypic Analysis. Proteinase and phospholipase activities were measured as described in (40) and (41), respectively. Melanin production and capsule size were measured as described in (42) and (43), respectively. Other enzymatic activities of *C. gattii* strains were tested with API-ZYM as described in (44).

Unless otherwise stated, statistical tests were performed by linear regression to test whether any of the tested phenotype was correlated with the intracellular proliferation rate.

ACKNOWLEDGMENTS. We thank Arturo Casadevall (Albert Einstein College of Medicine, Bronx, NY) for generously providing us with the 18B7 antibody, Marcus Harrison, Andrew Rogers and Volker Brenner at Oxford Gene Technology for assistance with the microarray analysis and James Kronstad and the Broad Institute for access to the unpublished WM276 and A1M-R265 genome sequences. This work was made possible with financial support from the Medical Research Council U.K. (grant G0601171) and the Rowbotham Bequest. F.H. is supported by the Odo van Vloten Foundation. We also would like to thank the Genetics Society (Heredity Fieldwork and Training Grants) and the Society of General Microbiology (President's Fund for Research Visits) for providing funding for Hansong Ma's research visit to the CBS to conduct the phenotypic analysis reported here.

1. Nguyen L, Pieters J (2005) The Trojan horse: Survival tactics of pathogenic mycobacteria in macrophages. *Trends Cell Biol* 15:269–276.
2. Pelchen-Matthews A, Raposo G, Marsh M (2004) Endosomes, exosomes, and Trojan viruses. *Trends Microbiol* 12:310–316.
3. Feldmesser M, Kress Y, Novikoff P, Casadevall A (2000) Cryptococcus neoformans is a facultative intracellular pathogen in murine pulmonary infection. *Infect Immun* 68:4225–4237.
4. Tucker SC, Casadevall A (2002) Replication of *Cryptococcus neoformans* in macrophages is accompanied by phagosomal permeabilization and accumulation of vesicles containing polysaccharide in the cytoplasm. *Proc Natl Acad Sci USA* 99:3165–3170.
5. Charlier C, et al. (2009) Evidence of a role for monocytes in dissemination and brain invasion by *Cryptococcus neoformans*. *Infect Immun* 77:120–127.
6. Chretien F, et al. (2002) Pathogenesis of cerebral *Cryptococcus neoformans* infection after fungemia. *J Infect Dis* 186:522–530.
7. Hull CM, Heitman J (2002) Genetics of *Cryptococcus neoformans*. *Annu Rev Genet* 36:557–615.
8. Kidd SE, et al. (2004) A rare genotype of *Cryptococcus gattii* caused the cryptococcosis outbreak on Vancouver Island (British Columbia, Canada). *Proc Natl Acad Sci USA* 101:17258–17263.
9. Byrnes EJ 3rd, Bildfell RJ, Dearing PL, Valentine BA, Heitman J (2009) Cryptococcus gattii with bimorphic colony types in a dog in western Oregon: Additional evidence for expansion of the Vancouver Island outbreak. *J Vet Diagn Invest* 21:133–136.
10. Byrnes EJ 3rd, et al. (2009) Molecular evidence that the range of the Vancouver Island outbreak of *Cryptococcus gattii* infection has expanded into the Pacific Northwest in the United States. *J Infect Dis* 199:1081–1086.
11. Kidd SE, Guo H, Bartlett KH, Xu J, Kronstad JW (2005) Comparative gene genealogies indicate that two clonal lineages of *Cryptococcus gattii* in British Columbia resemble strains from other geographical areas. *Eukaryot Cell* 4:1629–1638.
12. Fraser JA, et al. (2005) Same-sex mating and the origin of the Vancouver Island *Cryptococcus gattii* outbreak. *Nature* 437:1360–1364.
13. Liu OW, et al. (2008) Systematic genetic analysis of virulence in the human fungal pathogen *Cryptococcus neoformans*. *Cell* 135:174–188.
14. Shao X, et al. (2005) An innate immune system cell is a major determinant of species-related susceptibility differences to fungal pneumonia. *J Immunol* 175:3244–3251.
15. Kechichian TB, Shea J, Del Poeta M (2007) Depletion of alveolar macrophages decreases the dissemination of a glucosylceramide-deficient mutant of *Cryptococcus neoformans* in immunodeficient mice. *Infect Immun* 75:4792–4798.
16. Steen BR, et al. (2003) Cryptococcus neoformans gene expression during experimental cryptococcal meningitis. *Eukaryot Cell* 2:1336–1349.
17. Toffaletti DL, Del Poeta M, Rude TH, Dietrich F, Perfect JR (2003) Regulation of cytochrome c oxidase subunit 1 (COX1) expression in *Cryptococcus neoformans* by temperature and host environment. *Microbiology* 149:1041–1049.
18. Chen H, et al. (2003) Mitofusins Mfn1 and Mfn2 coordinately regulate mitochondrial fusion and are essential for embryonic development. *J Cell Biol* 160:189–200.
19. Chan DC (2006) Mitochondrial fusion and fission in mammals. *Annu Rev Cell Dev Biol* 22:79–99.
20. Karbowski M, et al. (2004) Quantitation of mitochondrial dynamics by photolabeling of individual organelles shows that mitochondrial fusion is blocked during the Bax activation phase of apoptosis. *J Cell Biol* 164:493–499.
21. Sugioka R, Shimizu S, Tsujimoto Y (2004) Fzo1, a protein involved in mitochondrial fusion, inhibits apoptosis. *J Biol Chem* 279:52726–52734.
22. Olson A, Stenlid J (2001) Plant pathogens. Mitochondrial control of fungal hybrid virulence. *Nature* 411:438.
23. Haag-Liautard C, et al. (2008) Direct estimation of the mitochondrial DNA mutation rate in *Drosophila melanogaster*. *PLoS Biol* 6:e204.
24. Denver DR, Morris K, Lynch M, Vassilieva LL, Thomas WK (2000) High direct estimate of the mutation rate in the mitochondrial genome of *Caenorhabditis elegans*. *Science* 289:2342–2344.
25. Lynch M, et al. (2008) A genome-wide view of the spectrum of spontaneous mutations in yeast. *Proc Natl Acad Sci USA* 105:9272–9277.
26. Litter J, Keszthelyi A, Hamari Z, Pfeiffer I, Kucsera J Differences in mitochondrial genome organization of *Cryptococcus neoformans strains*. *Antonie Van Leeuwenhoek* 88:249–255, 2005.
27. Bovers M, Hagen F, Kuramae EE, Boekhout T (2009) Promiscuous mitochondria in *Cryptococcus gattii*. *FEMS Yeast Res* 9:489–503.
28. Xu J, Yan Z, Guo H (2009) Divergence, hybridization, and recombination in the mitochondrial genome of the human pathogenic yeast *Cryptococcus gattii*. *Mol Ecol* in press.
29. Ichishita R, et al. (2008) An RNAi screen for mitochondrial proteins required to maintain the morphology of the organelle in *Caenorhabditis elegans*. *J Biochem* 143:449–454.
30. Narasipura SD, Chaturvedi V, Chaturvedi S (2005) Characterization of *Cryptococcus neoformans* variety *gattii* SOD2 reveals distinct roles of the two superoxide dismutases in fungal biology and virulence. *Mol Microbiol* 55:1782–1800.
31. Ingavale SS, et al. (2008) Importance of mitochondria in survival of *Cryptococcus neoformans* under low oxygen conditions and tolerance to cobalt chloride. *PLoS Pathog* 4:e1000155.
32. Toffaletti DL, Nielsen K, Dietrich F, Heitman J, Perfect JR (2004) Cryptococcus neoformans mitochondrial genomes from serotype A and D strains do not influence virulence. *Curr Genet* 46:193–204.
33. Halliday CL, Carter DA (2003) Clonal reproduction and limited dispersal in an environmental population of *Cryptococcus neoformans* var *gattii* isolates from Australia. *J Clin Microbiol* 41:703–711.
34. Fraser JA, Subaran RL, Nichols CB, Heitman J (2003) Recapitulation of the sexual cycle of the primary fungal pathogen *Cryptococcus neoformans* var. *gattii*: Implications for an outbreak on Vancouver Island, Canada *Eukaryot Cell* 2:1036–1045.
35. Ngamskulrungroj P, et al. (2008) Association between fertility and molecular sub-type of global isolates of *Cryptococcus gattii* molecular type VGII. *Med Mycol* 46:665–673.
36. Ma H, Croudace JE, Lammas DA, May RC (2006) Expulsion of live pathogenic yeast by macrophages. *Curr Biol* 16:2156–2160.
37. Fan W, Kraus PR, Boily MJ, Heitman J (2005) Cryptococcus neoformans gene expression during murine macrophage infection. *Eukaryot Cell* 4:1420–1433.
38. Stekel DJ (2003) in *Microarray Bioinformatics* (Cambridge Univ. Press, Cambridge), 1st Ed, p 280.
39. Benjamini Y, Hochberg Y (1995) Controlling the false discovery rate: A practical and powerful approach to multiple testing. *Journal-Royal Statistical Society Series B* 57:289.
40. Braga AA, de Morais PB, Linardi VR (1998) Screening of yeasts from Brazilian Amazon rain forest for extracellular proteinases production. *Syst Appl Microbiol* 21:353–359.
41. Vidotto V, et al. (1996) Phospholipase activity in *Cryptococcus neoformans*. *Mycopathologia* 136:119–123.
42. Rosas AL, Casadevall A (1997) Melanization affects susceptibility of *Cryptococcus neoformans* to heat and cold. *FEMS Microbiol Lett* 153:265–272.
43. Golubev VI, Manukian AR (1979) [Capsule formation in saprophytic yeasts]. (Translated from Russian) *Mikrobiologiia* 48:314–318.
44. Chen LC, Pirofski LA, Casadevall A (1997) Extracellular proteins of *Cryptococcus neoformans* and host antibody response. *Infect Immun* 65:2599–2605.
45. Chaturvedi S, Ren P, Narasipura SD, Chaturvedi V (2005) Selection of optimal host strain for molecular pathogenesis studies on *Cryptococcus gattii*. *Mycopathologia* 160:207–215.